Stefanovic, C., Morales-Céspedes, M., Róka, R. & García Armada, A. (06-09 September 2021). *Performance analysis of N-Fisher-Snedecor F fading and its application to N-Hop FSO communications* [proceedings]. 17th International Symposium on Wireless Communication Systems (ISWCS 2021), Berlin, Germany.

DOI: 10.1109/ISWCS49558.2021.9562137

Performance Analysis of N-Fisher-Snedecor $\mathcal{F}$ Fading and Its Application to N-Hop FSO Communications

Caslav Stefanovic*, Máximo Morales-Céspedes*, Rastislav Róka†, Ana García Armada*
*Department of Signal Theory and Communications
Universidad Carlos III de Madrid, 28911 Leganés, Spain
Emails: caslav.stefanovic@uc3m.es, mmcesped@ing.uc3m.es, anagar@ing.uc3m.es
†Slovak University of Technology
Institute of Multimedia Information and Communication Technologies
Ilkovičova 3, 812 19 Bratislava, Slovakia, Email: rastislav.roka@stuba.sk

***Abstract*—The Fisher-Snedecor $\mathcal{F}$ distribution has been recently proposed as an experimentally verified and tractable turbulence induced fading model (TIFM) for free space optical (FSO) communications. This paper provides outage probability (OP) and higher-order (HO) performance analysis of the product of N independent but not identically distributed (i.n.i.d) Fisher-Snedecor $\mathcal{F}$ random variates (RVs). Accurate and closed-form (C-F) expressions for cumulative distribution function (CDF), level crossing rate (LCR) and average fade duration (AFD) of N-Fisher-Snedecor $\mathcal{F}$ distribution are successfully derived. The general property of a Laplace approximation approach for evaluation of N-folded complex integral-form (I-F) LCR expressions has been applied. The obtained statistical results are directly related to the performance evaluation of N-hop FSO communication links over weak, moderate and strong atmospheric turbulence conditions.**

***Index Terms*—Fisher-Snedecor $\mathcal{F}$ distribution, FSO communications, Higher order statistics, Outage probability.**

I. Introduction

FSO communications are envisioned to be incorporated in emerging 5G and beyond 5G (B5G) communication systems [1]-[2]. FSO communications can provide many advantages in wireless communications. In particular, FSO links are cost effective and spectrum license free. Moreover, FSO communications provide large bandwidth and due to narrow beam widths, FSO communications can enable high level of security, interference immunity and increase energy efficiency of wireless transmission systems. On the other hand, atmospheric turbulence can drastically impact propagation during FSO transmission and can cause the system performance deterioration. Atmospheric weather conditions as well as pointing errors between transmitter and receiver are other relevant phenomena that can cause additional FSO system performance deterioration.

The Fisher-Snedecor $\mathcal{F}$ distribution has been recently proposed as an accurate and experimentally verified TIFM for FSO communications [3]. The Fisher-Snedecor $\mathcal{F}$ TIFM for FSO communications scenario with pointing errors in terms of the first-order statistical measures is considered in [4], whereas the hybrid mmWave/FSO transmission system over the Fisher-Snedecor $\mathcal{F}$ turbulence induced fading channel is addressed in [5]. The Fisher-Snedecor $\mathcal{F}$ distribution has been initially introduced in [6]. In [7], authors introduced cascaded N-Fisher-Snedecor $\mathcal{F}$ distribution modeled as the product of N independent but not identically distributed (i.n.i.d) RVs for feasible application in performance assessment of multi-hop relay communications. The first-order performance analysis of Fisher-Snedecor $\mathcal{F}$ fading distribution have been reported in [3]-[7].

The HO statistics of composite $\mathcal{F}$ fading model are provided in [8] while the HO measures of bivariate Fisher-Snedecor $\mathcal{F}$ RVs are considered in [9]. In order to get broader insight into the behaviour of FSO systems over rapidly time-variant turbulence induced fading channels, the HO statistical analysis is needed. Indeed, a level crossing rate (LCR) is time rate of change of the turbulence induced faded signal, while average fade duration (AFD) is the mean time of the turbulence induced faded signal being below a specified threshold. Moreover, the HO statistics provide useful knowledge of time-variant turbulence induced fading channels for a variety of 5G and beyond 5G FSO communication scenarios [10]-[11]. The HO performance measures over turbulence induced fading channels for FSO communications have been investigated in [12]-[14]. However, there are no reported results on LCR and AFD over N-Fisher-Snedecor $\mathcal{F}$ turbulence induced fading channels and its application to N-Hop FSO relay communications over weak, moderate and strong turbulence conditions.

This paper provides accurate and fast-computing, C-F HO statistical expressions such as LCR and AFD of N-Fisher-Snedecor $\mathcal{F}$ distribution obtained by general Laplace approximation method (GLAM). The obtained results for OP and HO statistics are related to the system performance of N-hop FSO amplify and forward relay communication system over N-Fisher-Snedecor $\mathcal{F}$ turbulence channels. Namely, we investigate the impact of the number of hops under weak, moderate and strong turbulence severity conditions on OP and HO performance measures of N-hop relay FSO system.

II. Fisher-Snedecor $\mathcal{F}$ Composite Fading Model

The recently introduced Fisher-Snedecor $\mathcal{F}$ TIFM for FSO communications can be modeled as the product of independent but not identically distributed (i.n.i.d) Gamma and normalized inverse Gamma (I-Gamma) random variates (RVs) [3]. The Fisher-Snedecor $\mathcal{F}$ fading model $Z_{\mathcal{F}}(t)$ can be written as:

$$Z_{\mathcal{F}}(t) = X_g(t)Y_{Ig}(t) = X_g(t)\frac{1}{Y_g(t)} \tag{1}$$

where $X_g(t)$ and $Y_{Ig}(t)$ are Gamma and normalized I-Gamma random processes (RPs), respectively. Since the normalized I-Gamma RV can be expressed as $Y_{Ig} = \frac{1}{Y_g}$, the probability density functions (pdfs) of X_g and Y_g are given as, respectively:

$$p_{X_g}(x_g) = \frac{(m_m/\Omega_m)^{m_m}}{\Gamma(m_m)}(x_g)^{m_m-1}e^{-\frac{m_m}{\Omega_m}(x_g)} \tag{2}$$

$$p_{Y_g}(y_g) = \frac{((m_s-1)/\Omega_s)^{m_s}}{\Gamma(m_s)}(y_g)^{m_s-1}e^{-\frac{(m_s-1)}{\Omega_s}(y_g)} \tag{3}$$

whose shape parameters are m_m and m_s, respectively, whereas the average powers are Ω_m and Ω_s, respectively. The $\Gamma(\cdot)$ is the Gamma function [15, Eq.(8.310.1)].

The pdf of $Z_{\mathcal{F}}$ can be obtained as:

$$p_{Z_{\mathcal{F}}}(z_{\mathcal{F}}) = \int_0^\infty \left|\frac{dx_g}{dz_{\mathcal{F}}}\right| p_{X_g}(z_{\mathcal{F}} \times y_g)p_{Y_g}(y_g)dy_g \tag{4}$$

where $\left|\frac{dx_g}{dz_{\mathcal{F}}}\right| = y_g$. After substitutions (2) and (3) in (4), and using transformations [15, Eq. (3.326.2)] and [15, Eq. (8.384.1)], respectively, the pdf of $Z_{\mathcal{F}}$ can be written as:

$$p_{Z_{\mathcal{F}}}(z_{\mathcal{F}}) = \frac{(\frac{m_m}{\Omega_m})^{m_m}(\frac{m_s-1}{\Omega_s})^{m_s}(\Omega_s\Omega_m)^{m_m+m_s}z_{\mathcal{F}}^{m_m-1}}{\beta(m_m,m_s)(\Omega_s m_m z_{\mathcal{F}} + \Omega_m(m_s-1))^{m_m+m_s}} \tag{5}$$

where $\beta(\cdot,\cdot)$ is the Beta function [15, Eq. (8.380.1)]. It can be observed that $p_{Z_{\mathcal{F}}}(z_{\mathcal{F}})$ in (5) for $\Omega_s = 1$, $\Omega_m = 1$, $m_m = a$ and $m_s = b$ reduces to the pdf of Fisher-Snedecor $\mathcal{F}$ distribution given by [3, Eq. (6)].

III. N-Fisher-Snedecor $\mathcal{F}$ Turbulence Induced Fading Model

The cascaded N-Fisher-Snedecor $\mathcal{F}$ TIFM can be modeled as the product of N i.n.i.d Gamma and normalized Gamma RPs:

$$Z_{\mathcal{F}_{out}}(t) = \prod_{i=1}^{N} Z_{\mathcal{F}_i}(t) = \prod_{i=1}^{N} X_{g,i}(t)Y_{Ig,i}(t) = \prod_{i=1}^{N}\frac{X_{g,i}(t)}{Y_{g,i}(t)} \tag{6}$$

where Gamma and normalized Gamma pdfs, $p_{X_{g,i}}(x_{g,i})$ and $p_{Y_{g,i}}(y_{g,i})$ are:

$$p_{X_{g,i}}(x_{g,i}) = \frac{a_i^{a_i}x_{g,i}^{a_i-1}}{\Gamma(a_i)}e^{-a_i x_{g,i}},\ i = 1, N \tag{7}$$

$$p_{Y_{g,i}}(y_{g,i}) = \frac{(b_i-1)^{b_i}y_{g,i}^{b_i-1}}{\Gamma(b_i)}e^{-(b_i-1)y_{g,i}},\ i = 1, N \tag{8}$$

The a_i and b_i are N-Fisher-Snedecor $\mathcal{F}$ small-scale and large-scale cells, respectively related to TIFM severity conditions. The scintillation index of N-Fisher-Snedecor $\mathcal{F}$ TIFM can be expressed as [3, Eq. (10)]:

$$\sigma^2_{Z_{\mathcal{F}_i}} = \left(1+\frac{1}{a_i}\right)\left(1+\frac{1}{b_i-2}\right) - 1,\ b_i > 2 \tag{9}$$

The a_i and b_i of N-Fisher-Snedecor $\mathcal{F}$ TIFM can be written as [4, Eq. (2)]:

$$a_i = \frac{1}{e^{\sigma^2_{lnX_{g,i}}}-1},\ b_i = \frac{1}{e^{\sigma^2_{lnY_{g,i}}}-1} + 2,\ i = 1, N \tag{10}$$

where $\sigma^2_{X_{g,i}}$ and $\sigma^2_{Y_{g,i}}$ are normalized log-irradiance variances of X_{g_i} and Y_{g_i}, respectively. Under the assumption of spherical propagation, the $\sigma^2_{lnX_{g,i}}$ is [4, Eq. (3)]:

$$\sigma^2_{lnX_{g,i}} = \frac{0.51\sigma^2_{SP,i}(1+0.69\sigma^{12/5}_{SP,i})^{-5/6}}{1+0.90d_i^2(\sigma_i/\sigma^2_{SP,i})^{12/5}+0.62d_i^2\sigma_i^{12/5}} \tag{11}$$

where $\sigma_{SP,i}$ represents i-th spherical scintillation index and by assuming further weak fluctuation conditions, $\sigma_{SP,i}$ is:

$$\begin{aligned}\sigma^2_{SP,i} = 9.65\sigma_i^2\Bigg(&0.4(1+9/Q_{l_i}^2)^{11/12}\Bigg[\sin(\frac{11}{6}\arctan\frac{Q_{l_i}}{3}) \\ &+ \frac{2.61}{(9+Q_{l_i}^2)^{1/4}}\sin(\frac{4}{3}\arctan\frac{Q_{l_i}}{3}) \\ &- \frac{0.52}{(9+Q_{l_i}^2)^{7/24}}\sin(\frac{5}{4}\arctan\frac{Q_{l_i}}{3})\Bigg] - 3.5/Q_{l_i}^{\frac{5}{6}}\Bigg)\end{aligned} \tag{12}$$

where $Q_{l_i} = 10.89L_i/(\beta_i l_{0_i}^2)$, L_i is i-th propagation distance, $\beta_i = 2\pi/\lambda_i$ is i-th wave-number (λ_i-wavelength) and l_{0_i} is i-th inner-scale. Furthermore, $d_i = \sqrt{\beta_i D_i^2/4L_i}$ and $\sigma_i^2 = 0.5C_{n_i}^2\beta_i^{7/6}L_i^{11/6}$ represents Rytov variance. D_i is i-th receiver aperture diameter and $C_{n_i}^2$ is i-th refractive index. The $\sigma^2_{lnY_{g,i}}$ can be written as [3, Eq. (15)]:

$$\sigma^2_{lnY_{g,i}} = \sigma^2_{lnY_{g,i}}(l_{0i}) - \sigma^2_{lnY_{g,i}}(L_{0i}) \tag{13}$$

where $\sigma^2_{lnY_{g,i}}(l_{0i})$ and $\sigma^2_{lnY_{g,i}}(L_{0i})$ are inner and outer large-scale log-irradiance variances, respectively that can be expressed as:

$$\begin{aligned}\sigma^2_{lnY_{g,i}} = 0.04\sigma_i^2(\frac{\eta_i(u_i)}{\eta_i(u_i)+Q_{l_i}})^{7/6}[1+1.75(\frac{\eta_i(u_i)}{\eta_i(u_i)+Q_{l_i}})^{1/2} \\ -(\frac{\eta_i(u_i)}{\eta_i(u_i)+Q_{l_i}})^{7/12}]\end{aligned} \tag{14}$$

where $u_i = \{l_{0_i}, L_{0_i}\}$. Additionally, $\eta_i(l_{0_i}) = \frac{8.56}{1+0.18d_i^2+0.20\sigma_i^2Q_{l_i}^{\frac{1}{6}}}$, $\eta_i(L_{0_i}) = \frac{Q_{0_i}\eta_i(l_{0_i})}{Q_{0_i}+\eta_i(l_{0_i})}$ and $Q_{0_i} = \frac{64\pi^2L_i}{\beta_i L_0^2}$.

A. Level Crossing Rate

Level crossing rate (LCR) of cascaded N-Fisher-Snedecor $\mathcal{F}$ distribution for a given threshold z_{th} can be written as:

$$N_{Z_{\mathcal{F}_{out}}}(z_{th}) = \int_0^{\infty} \dot{z}_{\mathcal{F}_{out}} p_{Z_{\mathcal{F}_{out}}\dot{Z}_{\mathcal{F}_{out}}}(z_{th}, \dot{z}_{\mathcal{F}_{out}}) d\dot{z}_{\mathcal{F}_{out}} \tag{15}$$

where, $p_{Z_{\mathcal{F}_{out}}\dot{Z}_{\mathcal{F}_{out}}}(z_{\mathcal{F}_{out}}, \dot{z}_{\mathcal{F}_{out}})$ is the joint distribution of $Z_{\mathcal{F}_{out}}$ and its first derivative $\dot{Z}_{\mathcal{F}_{out}}$. Based on (6), we can apply the following transformation:

$$X_{g,1} = \frac{Z_{\mathcal{F}_{out}} \prod_{i=1}^{N} Y_{g,i}}{\prod_{i=2}^{N} X_{g,i}} \tag{16}$$

Moreover, $p_{Z\,\mathcal{F}_{out}\dot{Z}_{\mathcal{F}_{out}}}(z_{\mathcal{F}_{out}}, \dot{z}_{\mathcal{F}_{out}})$ can be written as 2*N*-1 folded, I-F expression of the joint pdf of i.n.i.d RVs, $Z_{\mathcal{F}_{out}}, \dot{Z}_{\mathcal{F}_{out}}, Y_{g,1}, X_{g,2}, Y_{g,2}, \ldots, X_{g,N}$ and $Y_{g,N}$, as follows from [16, Eq. (12)]. The $p_{Z\,\mathcal{F}_{out}\dot{Z}_{\mathcal{F}_{out}}}(z_{\mathcal{F}_{out}}, \dot{z}_{\mathcal{F}_{out}})$ is given as (17) at the top of the next page, where $p_{Z_{\mathcal{F}_{out}}\dot{Z}_{\mathcal{F}_{out}}Y_{g,1}X_{g,2}\ldots X_{g,N}Y_{g,N}}$ can be expressed through conditional and individual pdfs [16, Eq. (13)]:

$$\begin{aligned}
&p_{Z_{\mathcal{F}_{out}}\dot{Z}_{\mathcal{F}_{out}}Y_{g,1}X_{g,2}\ldots Y_{g,N}}(z_{\mathcal{F}_{out}}\dot{z}_{\mathcal{F}_{out}}y_{g,1}x_{g,2}\ldots y_{g,N}) \\
&= p_{\dot{Z}_{\mathcal{F}_{out}}|Z_{\mathcal{F}_{out}}Y_{g,1}X_{g,2}\ldots Y_{g,N}}(\dot{z}_{\mathcal{F}_{out}}|z_{\mathcal{F}_{out}}y_{g,1}\ldots y_{g,N}) \\
&\times p_{Z_{\mathcal{F}_{out}}|Y_{g,1}X_{g,2}\ldots Y_{g,N}}(z_{\mathcal{F}_{out}}|y_{g,1}x_{g,2}\ldots y_{g,N}) \\
&\times p_{Y_{g,1}}(y_{g,1}) p_{X_{g,2}}(x_{g,2}) \ldots p_{Y_{g,N}}(y_{g,N})
\end{aligned} \tag{18}$$

The $p_{Z_{\mathcal{F}_{out}}|Y_{g,1}X_{g,2}\ldots Y_{g,N}}(z_{\mathcal{F}_{out}}|y_{g,1}x_{g,2}\ldots y_{g,N})$ with a help of (16) can be written as:

$$\begin{aligned}
&p_{Z_{\mathcal{F}_{out}}|Y_{g,1}X_{g,2}\ldots Y_{g,N}}(z_{\mathcal{F}_{out}}|y_{g,1}x_{g,2}\ldots y_{g,N}) \\
&= \left|\frac{dx_{g,1}}{dz_{\mathcal{F}_{out}}}\right| p_{X_{g,1}}\left(\frac{z_{\mathcal{F}_{out}} \prod_{i=1}^{N} y_{g,i}}{\prod_{i=2}^{N} x_{g,i}}\right)
\end{aligned} \tag{19}$$

From (15-19), $N_{Z_{\mathcal{F}_{out}}}(z_{th})$ can be written as (20), provided on the next page, where $\int_0^{\infty} \dot{z}_{\mathcal{F}_{out}} p_{\dot{Z}_{\mathcal{F}_{out}}|Z_{\mathcal{F}_{out}}\ldots Y_{g,N}}(\dot{z}_{\mathcal{F}_{out}}|z_{th}\ldots y_{g,N}) d\dot{z}_{\mathcal{F}_{out}}$ is the I-F expression and in the case of independent RVs can be evaluated as:

$$\begin{aligned}
&\int_0^{\infty} \dot{z}_{\mathcal{F}_{out}} p_{\dot{Z}_{\mathcal{F}_{out}}|Z_{\mathcal{F}_{out}}\ldots Y_{g,N}}(\dot{z}_{\mathcal{F}_{out}}|z_{th}\ldots y_{g,N}) d\dot{z}_{\mathcal{F}_{out}} \\
&= \frac{1}{\sqrt{2\pi}} \sigma_{\dot{Z}_{\mathcal{F}_{out}}}
\end{aligned} \tag{21}$$

The $\sigma^2_{\dot{Z}_{\mathcal{F}_{out}}}$ is the variance of $\dot{Z}_{\mathcal{F}_{out}}$. From (6), the first derivative of $Z_{\mathcal{F}_{out}}$ is:

$$\dot{Z}_{\mathcal{F}_{out}} = \prod_{i=1}^{N} Z_{\mathcal{F}_1} Z_{\mathcal{F}_2} \ldots Z_{\mathcal{F}_N} \left(\frac{\dot{Z}_{\mathcal{F}_1}}{Z_{\mathcal{F}_1}} + \frac{\dot{Z}_{\mathcal{F}_2}}{Z_{\mathcal{F}_2}} \ldots + \frac{\dot{Z}_{\mathcal{F}_N}}{Z_{\mathcal{F}_N}}\right) \tag{22}$$

We observe that the first derivatives of *N* zero-mean (Z-M) Gaussian (G) RVs $Z_{\mathcal{F}_1}, Z_{\mathcal{F}_2}, .., Z_{\mathcal{F}_N}$ denoted as, respectively $\dot{Z}_{\mathcal{F}_1}, \dot{Z}_{\mathcal{F}_2}, .., \dot{Z}_{\mathcal{F}_N}$ are also Z-M G RVs. Based on (22) and after some mathematical manipulations, the variance of $\dot{Z}_{\mathcal{F}_{out}}$ can be written as (23), given on the next page, where $\sigma^2_{\dot{Z}_{\mathcal{F}_i}}$, $i = 1, N$ are the variances of $\dot{Z}_{\mathcal{F}_i}, i = 1, N$, respectively. After substituting (21) in (20) and than (7), (8) in (20), the LCR of N-Fisher-Snedecor $\mathcal{F}$ distribution for a given threshold z_{th} is:

$$N_{Z_{\mathcal{F}_{out}}}(z_{th}) = \frac{1}{\sqrt{2\pi}} \prod_{i=1}^{N} \frac{a_i^{a_i}(b_i-1)^{b_i}}{\Gamma(a_i)\Gamma(b_i)} z_{th}^{a_1-1} E_1 \tag{24}$$

where, E_1 is 2*N*-1 folded, I-F expression provided as (25) on the next page. The C-F approximate $N_{Z_{\mathcal{F}_{out}}}(z_{th})$ expression is evaluated in the Appendix.

B. Average Fade Duration

Average fade duration (AFD) of N-Fischer-Snedecor $\mathcal{F}$ distribution can be defined as:

$$A_{Z_{\mathcal{F}_{out}}}(z_{th}) = \frac{F_{Z_{\mathcal{F}_{out}}}(z_{th})}{N_{Z_{\mathcal{F}_{out}}}(z_{th})} \tag{26}$$

where $F_{Z_{\mathcal{F}_{out}}}(z_{th})$ is the cdf of N-Fisher Snedecor $\mathcal{F}$ distribution for a given z_{th}. The cdf of N-Fisher-Snedecor $\mathcal{F}$ RP modeled as the product of N independent Nakagami-m and inverse Nakagami-m RPs has been recently provided in [7, Eq. (11)]. By applying the same analytical approach as in [7], the cdf of cascaded N-Fisher-Snedecor $\mathcal{F}$ distribution, modeled as the product of *N* i.n.i.d Gamma and normalized inverse Gamma RPs can be written as (27), provided in terms of the Meijer's G function [15, Eq. (9.301)] on the next page.

The received signal of one-hop FSO transmission link in the case of intensity modulation/direct detection (IM/DD) with on-off keying (OOK) technique of Fisher-Snedecor $\mathcal{F}$ TIFM can be written as [3, Eq. (19)]:

$$y_1 = x Z_{\mathcal{F}_1} R_{D,1} + n_1 \tag{28}$$

where the optical power can be represented by the optical intensity under the assumption that the area at reception is normalized to unity [3]. The x is transmitted information bit, $R_{D,1}$ is responsivity of the photo-detector, $Z_{\mathcal{F}_1}$ presents the Fisher-Snedecor $\mathcal{F}$ TIFM irradinace and n_1 is the AWGN. Moreover, the received signal of *i*-th link of extended N-hop FSO communications with *N*-1 amplify-and-forward relays is [17, Eq. (18)]:

$$y_i = s_{i-1} x Z_{\mathcal{F}_i} R_{D,i} y_{i-1} + n_i \tag{29}$$

where s_i is the fixed gain of *i*-th relay. Accordingly, the received signal at the destination of N-hop FSO relay link over Fisher-Snedecor $\mathcal{F}$ TIFM can be written as:

$$y_N = \prod_{i=1}^{N} s_{i-1} Z_{\mathcal{F}_i} R_{D,i} x + \sum_{i=1}^{N} n_i \prod_{j=i+1}^{N} s_{j-1} Z_{\mathcal{F}_j} R_{D,j} \tag{30}$$

$$p_{Z_{\mathcal{F}_{out}}\dot{Z}_{\mathcal{F}_{out}}}(z_{\mathcal{F}_{out}},\dot{z}_{\mathcal{F}_{out}}) = \int_0^\infty dx_{g,2}\ldots\int_0^\infty dx_{g,N}\int_0^\infty dy_{g,1}\int_0^\infty dy_{g,2}\ldots\int_0^\infty dy_{g,N} \times p_{Z_{\mathcal{F}_{out}}\dot{Z}_{\mathcal{F}_{out}}Y_{g,1}X_{g,2}\ldots X_{g,N}Y_{g,N}}(z_{\mathcal{F}_{out}}\dot{z}_{\mathcal{F}_{out}}y_{g,1}x_{g,2}\ldots x_{g,N}y_{g,N}) \tag{17}$$

$$N_{Z_{\mathcal{F}_{out}}}(z_{th}) = \int_0^\infty dx_{g,2}\int_0^\infty dx_{g,3}\ldots\int_0^\infty dx_{g,N}\int_0^\infty dy_{g,1}\int_0^\infty dy_{g,2}\ldots\int_0^\infty dy_{g,N} \times \left|\frac{dx_{g,1}}{dz_{\mathcal{F}_{out}}}\right| p_{X_{g,1}}\left(\frac{z_{th}\prod_{i=1}^N y_{g,i}}{\prod_{i=2}^N x_{g,i}}\right) p_{X_{g,2}}(x_{g,2})\ldots p_{X_{g,N}}(x_{g,N}) \times p_{Y_{g,1}}(y_{g,1})p_{Y_{g,2}}(y_{g,2})\ldots p_{Y_{g,N}}(y_{g,N})\int_0^\infty \dot{z}_{\mathcal{F}_{out}} p_{\dot{Z}_{\mathcal{F}_{out}}|Z_{\mathcal{F}_{out}}\ldots Y_{g,N}}(\dot{z}_{\mathcal{F}_{out}}|z_{th}\ldots y_{g,N})d\dot{z}_{\mathcal{F}_{out}} \tag{20}$$

$$\sigma^2_{\dot{Z}_{\mathcal{F}_{out}}} = \frac{y^2_{g,1}}{x^2_{g,1}}\prod_{i=1}^N\frac{x^2_{g,i}}{y^2_{g,i}}\sigma^2_{\dot{Z}_{\mathcal{F}_1}}\left(1+\frac{z^2_{\mathcal{F}_{out}}x^2_{g,1}y^2_{g,2}}{y^2_{g,1}x^2_{g,2}}\prod_{i=1}^N\frac{y^2_{g,i}}{x^2_{g,i}}\sigma^2_{\dot{Z}_{\mathcal{F}_2}}/\sigma^2_{\dot{Z}_{\mathcal{F}_1}} + \frac{z^2_{\mathcal{F}_{out}}x^2_{g,1}y^2_{g,3}}{y^2_{g,1}x^2_{g,3}}\prod_{i=1}^N\frac{y^2_{g,i}}{x^2_{g,i}}\sigma^2_{\dot{Z}_{\mathcal{F}_3}}/\sigma^2_{\dot{Z}_{\mathcal{F}_1}} \ldots + \frac{z^2_{\mathcal{F}_{out}}x^2_{g,1}y^2_{g,N}}{y^2_{g,1}x^2_{g,N}}\prod_{i=1}^N\frac{y^2_{g,i}}{x^2_{g,i}}\sigma^2_{\dot{Z}_{\mathcal{F}_N}}/\sigma^2_{\dot{Z}_{\mathcal{F}_1}}\right) \tag{23}$$

$$E_1 = \int_0^\infty dx_{g,2}\int_0^\infty dx_{g,3}\ldots\int_0^\infty dx_{g,N}\int_0^\infty dy_{g,1}\int_0^\infty dy_{g,2}\ldots\int_0^\infty dy_{g,N} \times x_{g,2}^{a_2-a_1-1}x_{g,3}^{a_3-a_1-1}\ldots x_{g,N}^{a_N-a_1-1}y_{g,1}^{b_1+a_1-1}y_{g,2}^{b_2+a_1-1}\ldots y_{g,N}^{b_N+a_N-1}\sigma_{\dot{Z}_{\mathcal{F}_{out}}} \times e^{-a_1\frac{z_{th}\prod_{i=1}^N y_{g,i}}{\prod_{i=2}^N x_{g,i}} - a_2x_{g,2} - a_3x_{g,3}\ldots - a_Nx_{g,N} - a_3x_{g,N} - (b_1-1)y_{g,1} - (b_2-1)y_{g,2}\ldots - (b_N-1)y_{g,N}} \tag{25}$$

$$F_{Z_{\mathcal{F}_{out}}}(z_{\mathcal{F}_{out}}) = \frac{1}{\prod_{i=1}^N\Gamma(a_i)\Gamma(b_i)}G_{N,N+1}^{N+1,N+1}\left(z_{\mathcal{F}_{out}}\prod_{i=1}^N\frac{a_i}{(b_i-1)}\middle|\begin{matrix}1-b_1,1-b_2,...,1-b_N,1\\ a_1,a_2,...,a_N,0\end{matrix}\right) \tag{27}$$

Based on (30), the total channel gain is $S = \prod_{i=1}^N s_{i-1}Z_{\mathcal{F}_i}R_{D,i}$. Furthermore, the received signal-to-noise ratio (SNR) of *i*-th link and average signal-to-noise ratio (SNR) of *i*-th link of the considered model are, respectively, $\gamma_{Z_{\mathcal{F}_i}} = \frac{R^2_{D,i}z^2_{\mathcal{F}_i}}{N_{0_i}}$, $\Omega_{\mathcal{F}_i} = \frac{R^2_{D,i}(\langle z_{\mathcal{F}_i}\rangle)^2}{N_{0_i}}$, where N_{0_i} is noise power of *i*-th link. Without loss of generality and in accordance with some previous works we define $s_0 = s_i = 1$ [17]. Under the assumption that the faded signal of *N* hop FSO relay link can be directly estimated at destination, the N-Fisher-Snedecor $\mathcal{F}$ faded signal at reception can be considered as cascaded one as in [17].

IV. Numerical Results

Numerical results for OP and HO statistical measures of N-Fisher-Snedecor $\mathcal{F}$ distribution under weak ($a_i = 4.5916$, $b_i = 7.0941$), moderate ($a_i = 2.3378$, $b_i = 4.5323$) and strong ($a_i = 1.4321$, $b_i = 3.4948$) TIFM conditions are presented in Figs. 1-3, respectively. It can be noticed that the approximate C-F expressions for LCR and AFD fit well with the exact I-F expressions, especially for higher thresholds.

Fig. 1 presents OP of N-Fisher-Snedecor $\mathcal{F}$ distribution. The OP is obtained by $P_{out}(\nu_{th}) = P_{out}(\nu \leq \nu_{th}) = F_{Z_{\mathcal{F}_{out}}}(\nu_{th}^{-1/2})$ where the SNR threshold at the output is defined as $\nu_{th} = \prod_{i=1}^N \nu_{th_i}$, whereas $\nu_{th_i} = \frac{R^2_{D,i}}{\gamma_{Z_{\mathcal{F}_i}}N_{0_i}}$. It can be observed that $P_{out}(\nu_{th})$ takes smaller values for smaller number of hops (e.g., by decreasing number of hops from *N*=1 to *N*=3) and by shifting from strong-to-weak N-Fisher-Snedecor $\mathcal{F}$ TIFM severity conditions. Moreover, Fig. 1 shows that the results for $P_{out}(\nu_{th})$ for *N*=1 and under weak turbulence severity conditions coincide with the reported results for OP of Fisher-Snedecor $\mathcal{F}$ distribution [3].

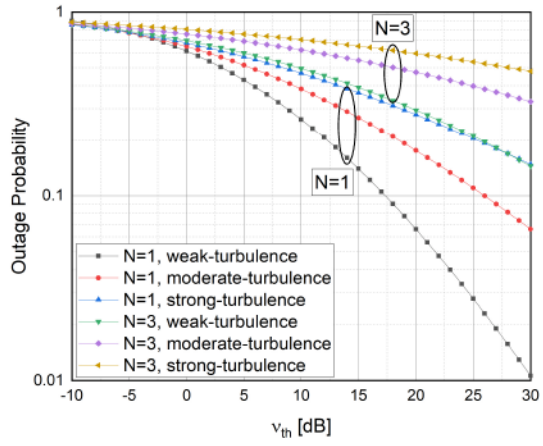

Fig. 1. Outage Probability of N-Fisher-Snedecor $\mathcal{F}$ TIFM observed for weak, moderate and strong turbulence conditions and various N.

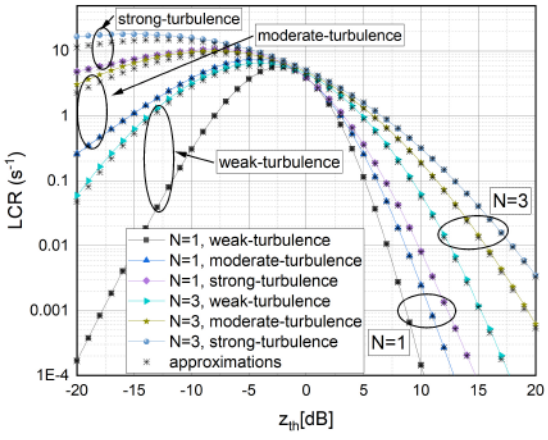

Fig. 2. LCR (s^{-1}) of N-Fisher-Snedecor $\mathcal{F}$ TIFM observed for weak, moderate and strong turbulence conditions and various N.

Fig. 2 shows $N_{Z_{\mathcal{F}_{out}}}(z_{th})$. The variances in (23) are evaluated as $\sigma^2_{Z_{\mathcal{F}}} = \sigma^2_{Z_{\mathcal{F}_i}} = {f_{0_i}}^2\pi^2\sigma^2_{Z_{\mathcal{F}_{N_i}}}\langle z_{\mathcal{F}_i}\rangle$ [12, Eq. (13)], where $\langle z_{\mathcal{F}_i}\rangle = 1$. Furthermore, the $f_{0_i} = \frac{1}{\pi\tau_{0_i}\sqrt{2}}$ is quasi frequency of the i-th FSO path [12, eq. (15)]. Additionally, $\tau_{0,i} = \frac{\sqrt{\lambda_i L_i}}{U_i}$ is turbulence correlation time, λ_i is the wavelength, L_i is optical propagation distance and U_i is average wind speed of the i-th transmission link. As expected, strong turbulence causes $N_{Z_{\mathcal{F}_N}}(z_{th})$ to take higher values. By shifting from strong-to-moderate or moderate-to-weak turbulence conditions, $N_{z_{\mathcal{F}_N}}(z_{th})$ decreases. Contrary, the increase in the value of N causes $N_{Z_{\mathcal{F}_N}}(z_{th})$ to increase. It can be further noticed that for lower z_{th} dB values, N-Fisher-Snedecor $\mathcal{F}$ TIFM severity conditions have stronger impact on $N_{z_{\mathcal{F}_N}}(z_{th})$ than N, while for higher z_{th} dB values, the number of hops has stronger impact on $N_{Z_{\mathcal{F}_N}}(z_{th})$ than N-Fisher-Snedecor $\mathcal{F}$ TIFM severity conditions.

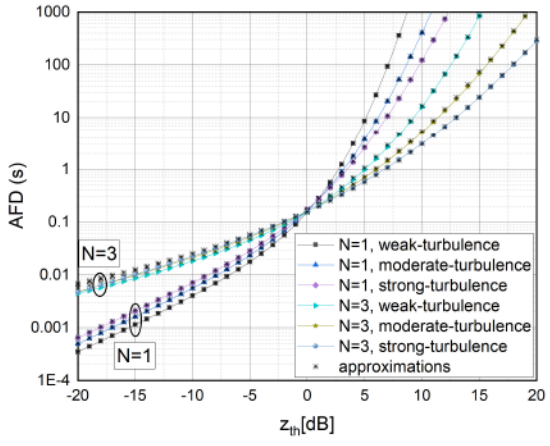

Fig. 3. AFD (s) of N-Fisher-Snedecor $\mathcal{F}$ TIFM observed for weak, moderate and strong turbulence conditions and various N.

The $A_{Z_{\mathcal{F}_N}}(z_{th})$ for weak, moderate and strong turbulence conditions and different values of N of cascaded N-Fisher-Snedecor $\mathcal{F}$ distribution is presented in Fig. 3. It can be seen that by increasing the value of N (e.g., by increasing from N=1 to N=3), the $A_{Z_{\mathcal{F}_N}}(z_{th})$ increases for lower threshold values while $A_{Z_{\mathcal{F}_N}}(z_{th})$ decreases for higher threshold values. It can be further observed that by shifting from strong-to-moderate or moderate-to-weak N-Fisher-Snedecor $\mathcal{F}$ TIFM conditions, $A_{Z_{\mathcal{F}_N}}(z_{th})$ slightly decreases for lower threshold values.

The $N_{Z_{\mathcal{F}_i}}(z_{th})$ and $A_{Z_{\mathcal{F}_N}}(z_{th})$ in Figs. 2-3 are presented for the following system parameters of each FSO link ($\lambda = \lambda_i = 850\,nm$, $U = U_i = 1\,m/s$ and $L = L_i = 500\,m$).

V. Conclusion

The paper provides novel C-F expressions for OP, LCR and AFD of N-Fisher-Snedecor $\mathcal{F}$ distribution. The accurate and fast-computing HO statistical C-F approximate results are fitting well with the exact I-F results. In general, the system performance improvement in lower dB output threshold regime can be achieved by shifting from strong-to-weak TIFM severity conditions and by decreasing number of hops.

Appendix

The general Laplace approximation formula (GLAF) has been initially proven by authors in [18], whereas in [16] authors have applied the GLAF for the cases where real-valued parameter γ takes small values. The GLAF that can be used to evaluate 2N-1 I-F expression is [16, Eq. (I.3)]:

$$\int_0^\infty dx_{g,2}\int_0^\infty dx_{g,3}\ldots\int_0^\infty dx_{g,N} \times \int_0^\infty dy_{g,1}\int_0^\infty dy_{g,2}\ldots\int_0^\infty dy_{g,N-1} \times \int_0^\infty f_1(y_{g,1}, x_{g,2}, y_{g,2}, \ldots, x_{g,N}, y_{g,N})$$

$$h = \begin{bmatrix} \frac{\partial^2 f_2(y_{g,1},x_{g,2},\ldots,x_{g,N},y_{g,N})}{\partial y_{g,1}^2} & \frac{\partial^2 f_2(y_{g,1},x_{g,2},\ldots,x_{g,N},y_{g,N})}{\partial y_{g,1}\partial x_{g,2}} \cdots & \frac{\partial^2 f_2(y_{g,1},x_{g,2},\ldots,x_{g,N},y_{g,N})}{\partial y_{g,1}\partial y_{g,N}} \\ \frac{\partial^2 f_2(y_{g,1},x_{g,2},\ldots,x_{g,N},y_{g,N})}{\partial x_{g,2} y_{g,1}} & \frac{\partial^2 f_2(y_{g,1},x_{g,2},\ldots,x_{g,N},y_{g,N})}{\partial x_{g,2}^2} \cdots & \frac{\partial^2 f_2(y_{g,1},x_{g,2},\ldots,x_{g,N},y_{g,N})}{\partial x_{g,2}\partial y_{g,N}} \\ \vdots & \vdots & \vdots \\ \frac{\partial^2 f_2(y_{g,1},x_{g,2},\ldots,x_{g,N},y_{g,N})}{\partial y_{g,N}\partial y_{g,1}} & \frac{\partial^2 f_2(y_{g,1},x_{g,2},\ldots,x_{g,N},y_{g,N})}{\partial y_{g,N}\partial x_{g,2}} \cdots & \frac{\partial^2 f_2(y_{g,1},x_{g,2},\ldots,x_{g,N},y_{g,N})}{\partial y_{g,N}^2} \end{bmatrix} \tag{33}$$

$$\begin{aligned} &\times e^{-\gamma f_2(y_{g,1},x_{g,2},y_{g,2},\ldots,x_{g,N},y_{g,N})} dy_{g,N} \\ &\approx (\frac{2\pi}{\gamma})^{\frac{2N-1}{2}} \frac{f_1(\tilde{y}_{g,1},\tilde{x}_{g,2},\tilde{y}_{g,2},\ldots,\tilde{x}_{g,N},\tilde{y}_{g,N})}{\sqrt{det(\tilde{h})}} \\ &\times e^{-\gamma f_2(\tilde{y}_{g,1},\tilde{x}_{g,2},\tilde{y}_{g,2},\ldots,\tilde{x}_{g,N},\tilde{y}_{g,N})} \end{aligned} \tag{31}$$

where $f_1(y_{g,1}, x_{g,2}, y_{g,2}, \ldots, x_{g,N}, y_{g,N})$ and $f_2(y_{g,1}, x_{g,2}, y_{g,2}, \ldots, x_{g,N}, y_{g,N})$ are multi-variate functions of $y_{g,1}, x_{g,2}, y_{g,2}, \ldots, x_{g,N}$ and $y_{g,N}$, whereas γ is a real-valued parameter. The $\tilde{y}_{g,1}, \tilde{x}_{g,2}, \tilde{y}_{g,2}, \ldots, \tilde{x}_{g,N}$ and $\tilde{y}_{g,N}$ are real and positive values obtained from the set of 2*N*-1 differential equations,

$$\begin{aligned} &\frac{\partial f_2(y_{g,1}, x_{g,2}, y_{g,2}, \ldots, x_{g,N}, y_{g,N})}{\partial y_{g,1}} = 0, \\ &\frac{\partial f_2(y_{g,1}, x_{g,2}, y_{g,2}, \ldots, x_{g,N}, y_{g,N})}{\partial x_{g,2}} = 0, \\ &\vdots \\ &\frac{\partial f_2(y_{g,1}, x_{g,2}, y_{g,2}, \ldots, x_{g,N}, y_{g,N})}{\partial y_{g,N}} = 0 \end{aligned} \tag{32}$$

for $y_{g,i} = \tilde{y}_{g,i}, i = 1, N$ and $x_{g,i} = \tilde{x}_{g,i}, i = 2, N$. The $\tilde{h}$ is Hessian $(2N-1) \times (2N-1)$ matrix obtained from h in (33) for $y_{g,i} = \tilde{y}_{g,i}, i = 1, N$ and $x_{g,i} = \tilde{x}_{g,i}, i = 2, N$.

By applying (31-33) in (24), an C-F approximate LCR expression of N-Fisher-Snedecor $\mathcal{F}$ distribution is derived and numerically evaluated for γ=1.

ACKNOWLEDGMENT

The authors would like to acknowledge the CONEX-Plus project, the Spanish National Project TERESA-ADA (TEC2017-90093-C3-2-R) (MINECO/AEI/FEDER, UE), the KEGA 034STU-4/2021 "Utilization of Web-based Training and Learning Systems at the Development of New Educational Programs in the Area of Optical Wireless Technologies" and the Cost Action CA19111. The CONEX-Plus has received research funding from UC3M and the European Union's Horizon 2020 programme under the Marie Skłodowska-Curie grant agreement No 801538.

REFERENCES

[1] M. Alzenad, M. Z. Shakir, H. Yanikomeroglu and M. Alouini, "FSO-Based Vertical Backhaul/Fronthaul Framework for 5G+ Wireless Networks",*IEEE Communications Magazine*, vol. 56, no. 1, pp. 218–224, 2018.

[2] R. Róka, "Enhanced simulation tools for analyzing signal processing techniques in the optical transmission path," *Handbook of Research on 5G Networks and Advancements in Computing, Electronics and Electrical Engineering*, A. Nwajana (Ed.), I. Ihiane (Ed.). IGI Global, Hershey, USA, 2021. DOI: 10.4018/978-1-7998-6992-4

[3] H. P. Peppas, G. C. Alexandropoulos, E. D. Xenos and A. Maras, "The Fischer–Snedecor $\mathcal{F}$-Distribution Model for Turbulence-Induced Fading in Free-Space Optical Systems", *Journal of Lightwave Technology*, vol. 38, no. 6, pp. 1286–1295, 2020.

[4] O. S. Badarneh, R. Derbas, F. S. Almehmadi, F. El Bouanani and S. Muhaidat, "Performance Analysis of FSO Communications Over F Turbulence Channels With Pointing Errors", *IEEE Communications Letters*, vol. 25, no. 3, pp. 926–930, 2021.

[5] O. S. Badarneh and R. Mesleh, "Diversity analysis of simultaneous mmWave and free-space-optical transmission over F-distribution channel models", *Journal of Optical Communications and Networking*, vol. 12, no. 11, pp. 324–334, 2020.

[6] M. K. Yoo, S. L. Cotton, P. C. Sofotasios, M. Matthaiou, M. Valkama and G. K. Karagiannidis, "The Fisher–Snedecor $\mathcal{F}$ Distribution: A Simple and Accurate Composite Fading Model", *IEEE Communications Letters*, vol. 21, no. 7, pp. 1661–1664, 2017.

[7] O. S. Badarneh, S. Muhaidat, P. C. Sofotasios, S. L. Cotton and D. B. da Costa, "The N Fisher-Snedecor F cascaded fading model", *In 2018 14th International Conference on Wireless and Mobile Computing, Networking and Communications (WiMob)*, pp. 1–7, 2018.

[8] S. K. Yoo, S. L. Cotton, P. C. Sofotasios, S. Muhaidat and G. K. Karagiannidis, "Level Crossing Rate and Average Fade Duration in F Composite Fading Channels", *IEEE Wireless Communications Letters*, vol. 9, no. 3, pp. 281–284, 2020.

[9] W. Cheng and X. Wang, "Bivariate Fisher–Snedecor F Distribution and its Applications in Wireless Communication Systems", *IEEE Access*, vol. 8, pp. 146342–146360, 2020.

[10] H. D. Le and A. T. Pham, "Level Crossing Rate and Average Fade Duration of Satellite-to-UAV FSO Channels", *IEEE Photonics Journal*, vol. 13, no. 1, pp. 1–14, 2021.

[11] C. Stefanovic, M. Pratesi and F. Santucci, "Second order statistics of mixed RF-FSO relay systems and its application to vehicular networks", *IEEE International Conference on Communications (ICC)*, pp. 1-6, 2019.

[12] A. Jurado-Navas, J. M. Garrido Balsells, M. Castillo-Vazquez, I. Puerta-Notario, I. T. Monroy and J. J. V. Olmos, "Fade statistics of M-turbulent optical links", *EURASIP Journal on Wireless Communications and Networking*, (2017) 2017:112, DOI:10.1186/s13638-0170898-z.

[13] C. B. Issaid and M. S. Alouini, "Level Crossing Rate and Average Outage Duration of Free Space Optical Links", *IEEE Transactions on Communications*, vol. 67, no. 9, pp. 6234–6242, 2019.

[14] C. Stefanovic et al. "On the second order statistics of N-hop FSO communications over N-gamma-gamma turbulence induced fading channels," *Physical Communication*, p.101289, 2021.

[15] I. S. Gradshteyn and I. M. Ryzhik, *Table of Integrals, Series, and Products*, New York: Academic, 2000.

[16] Z. Hadzi-Velkov, Z. N. Zlatanov and G. K. Karagiannidis, "On the second order statistics of the multihop Rayleigh fading channel", *IEEE Transactions on Communications*, vol. 57, no. 6, pp. 1815–1823, 2009.

[17] C. K. Datsikas, K. P. Peppas, N. C. Sagias and G. S. Tombras, "Serial Free-Space Optical Relaying Communications Over Gamma-Gamma Atmospheric Turbulence Channels", *IEEE/OSA Journal of Optical Communications and Networking*, vol. 2, no. 8, pp. 576–586, 2010.

[18] L. C. Hsu, "A Theorem on the Asymptotic Behavior of a Multiple Integral", *Duke Mathematical Journal*, pp. 623–632, 1948.